JOC The Journal of Organic Chemistry

Article

pubs.acs.org/joc

# Ligand-Assisted Acyl Migration in Au-Catalyzed Isomerization of Propargylic Ester to Diketone: A DFT Study

Animesh Ghosh, Atanu Basak, Kuheli Chakrabarty, Boyli Ghosh, and Gourab Kanti Das*

Department of Chemistry, Visva-Bharati, Santiniketan 731235, West Bengal, India

Supporting Information

**ABSTRACT:** Gold-catalyzed isomerization of propargylic ester to a diketone derivative is a fascinating example for the generation of the C−C bond in organoaurate chemistry as it is one of the few reactions that exploit the nucleophilicity of organoaurates to a migrating acyl group. The proposed mechanistic pathway, involving the formation of a four-membered intermediate, has never been substantiated by any theoretical or experimental evidence. Detailed theoretical calculation suggests that the formation of an alkylideneoxoniumcyclobutene intermediate is highly unlikely. Instead, an acyl migration, assisted by the chlorine ligand in the square planar geometry of metal complex offers an alternative mechanism that can justify the reasonable activation barrier and the associated stereochemical feature involved in the reaction. The initial mandatory steps of the catalytic process such as allene formation (af) and rotamerization of allene-bound gold complex (ra) are found to be quite facile. However, the final step, acyl migration (am), that takes place through the formation of an intermediate with C−Cl bond, acts as the rate-determining step of the reaction. The mechanism also justifies the lack of sufficient activity of Au(I) salt to catalyze the isomerization process.

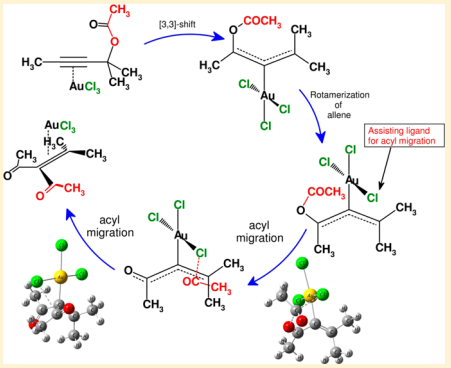


## INTRODUCTION

[1,3] shifting of an acyl group from the oxygen to the carbon atom in an −O−C═C− skeleton is not a common process in aliphatic organic compounds.[1] Such a process was detected in carboxyallene[2] intermediate by Wang and Zhang while studying the isomerization of propargylic esters in the presence of gold metal ion to generate a diketone derivative.[3]

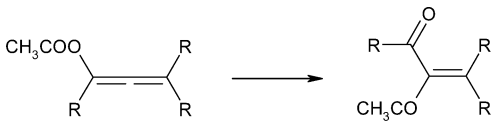


The authors observed that a propargylic ester when heated at 80 °C in the presence of $AuCl_3$ in toluene, smoothly isomerizes to the $\alpha$-alkylidene-$\beta$-diketone and the process was identified to be intramolecular in nature.

It is established that under the gold(I) or gold(III) catalytic conditions,[4] the propargylic esters generally undergo an initial [2,3] or [3,3] sigmatropic rearrangement.[5] Though the interconversion between the [2,3] or [3,3] rearranged product is shown to be reversible,[6] the proportion of these species in the equilibrating mixture largely depends on the steric and electronic nature of the substituents.[7] Literature survey reveals that the propargylic ester with a terminal alkyne favors the formation of a gold vinyl carbenoid system through [2,3] sigmatropic migration,[8] whereas alkynes with electron-rich substituents prefer [3,3] rearrangement to generate a gold-bound allene intermediate.[9] Depending on the nature of the substituent present in the reactant, the intermediates, generated from propargylic ester derivatives, finally evolve several isomerized cyclic or acyclic systems.[8,10] Though many of the reactions express the electrophilic nature of the gold allene complex some reports show that the intermediate has sufficient nucleophilic character to undergo addition to soft electrophiles.[11] However, experimental reports from other sources result some contradictory conclusion making it difficult to judge the actual role of metal ion in the reaction.[12]

Based on the previous facts on structural alteration of propargylic ester under the catalytic condition of gold salt, a mechanistic pathway (Scheme 1) for the formation of diketone from propargylic ester was proposed by the authors.[3] In this mechanism, the initially formed gold complex of the propargylic ester is converted to carboxyallene intermediate through the most accepted [3,3] sigmatropic rearrangement. The final acyl group migration was considered to occur through a tetrahedral four membered species that finally undergoes the ring-opening to form the isolable diketone derivative as the major product.

Though the hypothetical pathway explains qualitatively the overall process, it does not have sufficient transparency to explain several associated facts observed during the critical study of the rearrangement process. Variation of gold salt reveals that though Au(III) ion catalyzes smoothly the formation of diketone derivative, Au(I) complexes were found to be largely ineffective to catalyze the reaction. Requirement of specific oxidation state of the metal atom in such reaction is generally difficult to

**Received:** April 12, 2014
**Published:** May 19, 2014





dx.doi.org/10.1021/jo500822v | J. Org. Chem. 2014, 79, 5652−5663

**Scheme 1**

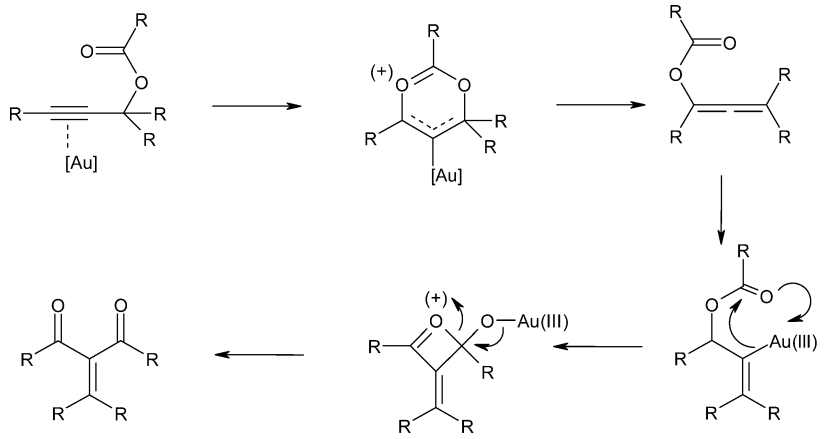


explain.[13] Moreover, variation of the substrate structure shows a strong preference for the *E* selectivity, which decreases with prolonged reaction time.[14] Critical analysis of such stereoselectivity suggests that the migrating acyl group requires some specific orientation relative to the metal bound nucleophile to produce the *E*-isomer in major amount. Inability of the existing mechanism to put forward a clear explanation for the dependence on the metal oxidation state and the preference for *E*-selectivity of the overall reaction caught our attention and tempted us to carry out a detailed theoretical investigation on a variety of possible pathways through which the reaction may occur.

Our observation reveals that, although the initial transformation of propargylic ester to the carboxyallene derivative takes place under the usual [3,3] sigmatropic rearrangement process, the generation of the diketone skeleton requires a specific conformational orientation of the gold-bound allene intermediate to make a suitable reaction pathway with the observed stereoselectivity. We surmised that such spatial orientation can be achieved through the conformation scrambling of the in situ generated metal-bound allene complex.[15]

Previous studies showed that the gold−allene complex may exist in several geometrical arrangements and can be categorized broadly in two classes.[16] The first category falls under the $\eta^2$ complex in which any one of the two orthogonal double bonds of the allene system coordinates to the metal atom and the distances between the metal and the coordinating carbon atoms depend on the nature of the substituent present on the allene moiety.[17] However, the second category that belongs to the $\eta^1$ complex involves the co-ordination between the central carbon atom of the allenic system and the metal ion.[18]


Though the first species may express the chiral nature of the allene system, the second one may exist in the chiral or achiral conformation. The chirality of the $\eta^1$ system is developed from the helical bent structure, which is important for many asymmetric syntheses to transfer the chirality of allene in the end product (axis-to-center chirality transfer).[15,19] Previous study reveals that all the species involved in the allene−Au complex are connected by low-lying transition states, which allow the conformational scrambling and generate a suitable structure that may assist the next step of our investigation.

After achieving such a suitable arrangement in the gold−allene complex, the chlorine ligand of the metal ion then assists the migration of the acyl group to generate the final skeleton of the product by forming C−C bond. We observed that the participation of the chlorine ligand for assisting the process will not only reduce down the activation barrier but also signify the importance of the square planar geometry of Au(III) complex, which is not possible with the linear geometry of Au(I) ion.

## COMPUTATIONAL METHODS

Guided by our previous experience,[20] we have chosen hybrid density functional PBE0[21] (equivalent to PBE1PBE) as a method for performing DFT calculations. The basis set double-$\zeta$ with the electron core potential LANL2[22] was employed to carry out the electronic structure calculation of Au, while other atoms are computed using the 6-31G(d,p) basis set.[23] Locating transition structures on the potential energy surfaces of several pathways has been found to be a difficult job when Au(III) metal is involved. The relatively shallow energy barrier for many conformational changes of the organoaurate derivatives and the extended nearly planar surface around the transition structures make it difficult to guess the trial geometries for locating the saddle points. Almost all the pathways involved in the conformational change of the organoaurate species were traced by the relaxed surface scan using redundant coordinate of the species. In many cases, the final confirmation of the transition structure for relating the corresponding reactant and product were performed by optimizing the geometries obtained by displacing manually the atoms along the two directions of the eigenvectors associated with the low imaginary frequency of normal vibrational modes of the species. Imaginary frequencies with relatively large value respond to the standard IRC procedure to relate the reactant and product. Solvent effect was approximated by introducing a polarizable continuum model (PCM),[24] and bulk solvent effects were computed using the gas phase optimized geometries. We have employed the standard parameters for the solvent toluene as this solvent was used to carry out the reaction experimentally. Solvation free energies were calculated by adding the solvation energies to the computed gas-phase relative free energies ($\Delta G_{353K}$). The relative energies were calculated with respect to the energy sum of free reactant and catalyst. All these calculations were performed using Gaussian-09 software.[25] While calculating the activation barrier, we pay special attention to the effect of dispersion energy of the species that are responsible in determining the energy barrier of the rate limiting and the overall processes. To include the dispersion correction factors we have employed the Grimme's DFT-D3[26] procedure with the short-range Becke-Johnson damping scheme.[27] Our finding reveals that selection of a favorable pathway from various mechanisms is not affected by the incorporation of dispersion correction of energies associated with the structures.


dx.doi.org/10.1021/jo500822v | J. Org. Chem. 2014, 79, 5652−5663

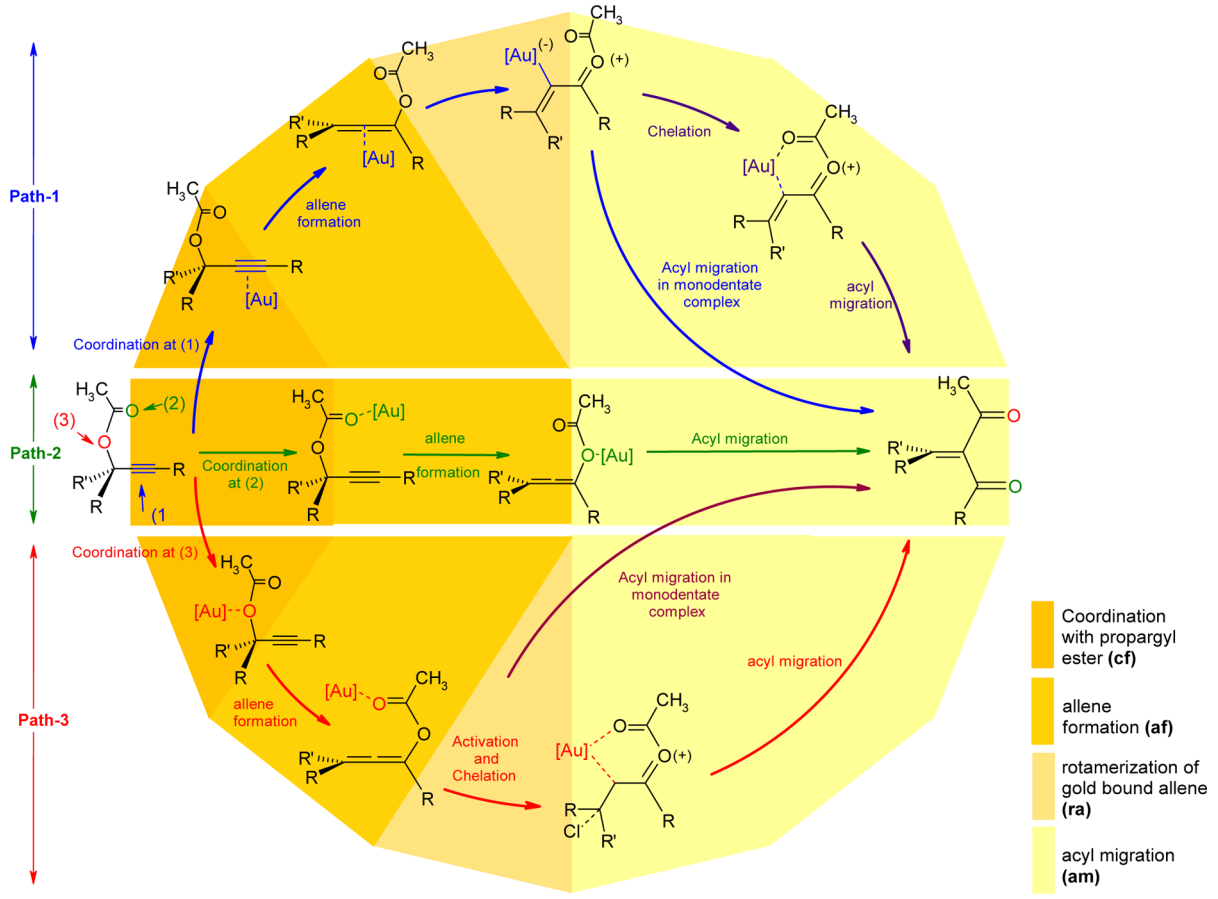


**Figure 1.** Overview of the possible mechanistic pathways.

**Table 1. Comparison of Energy Barrier of the Several Segments of Different Pathways and the Global Activation Energy (kcal mol$^{-1}$)**

| pathway | rel energy of the initially formed Au complex | maximum activation barrier in several segments in each pathway: allene formation (af) | rotamerization of allene (ra) | acyl migration (am) | global activation barrier | rel energy of the highest transition structure |
|---|---|---|---|---|---|---|
| dimethyl derivative (D) | | | | | | |
| path 1 (Figure 2) (monodentate) | −39.78 | 12.63 | 10.47 | 20.08 (18.87)[a] | 25.50 (22.58) | −32.09 (−41.52) |
| path 1 (Figure.SI-3) (bidentate) | −39.78 | 12.63 | 10.47 | 42.30 (43.07) | 47.72 (46.78) | −9.87 (−17.32) |
| path 2 (Figure.SI-4) (monodendate) | −37.41 | 32.71 | | 25.60 (25.91) | 32.71 (30.29) | −4.70 (−11.76) |
| path 3 (Figure.SI-5) (monodentate) | −26.47 | 18.87 | | 30.99 (29.86) | 30.99 (29.86) | −7.60 (−14.21) |
| path 3(Figure.SI-6) (bidentate) | −26.47 | 18.87 | | 38.86 (34.63) | 38.86 (34.63) | −2.52 (−9.44) |
| trimethyl derivative (T) | | | | | | |
| path 1 (Figure 3) | −44.18 | 6.88 | 0.57 | 19.81 (18.23) | 26.20 (23.57) | −35.45 (−45.21) |
| path 1 (Figure.SI-8) (bidentate) | −44.18 | 6.88 | 0.57 | 37.20 (37.54) | 43.59 (42.88) | −18.06 (−25.10) |
| path 2 (Figure.SI-9) | −41.17 | | | 21.29 (20.96) | not less than 30.20 (28.65) | not less than −10.97 (−16.94) |
| path 3 (Figure.SI-10) (monodentate) | −32.80 | | | 27.04 (27.31) | not less than 27.04 (27.31) | not less than −15.99 (−21.95) |
| path 3 (Figure.SI-11) (bidentate) | −32.80 | | | 37.05 (35.51) | not less than 37.05 (35.51) | not less than −17.90 (−26.88) |

[a]Activation barriers shown in parentheses are calculated after incorporation of the dispersion correction terms.

## RESULTS AND DISCUSSION

### Designed Pathways and the Comparison of Energetic.

Selected model structures of the methyl-substituted propargylic esters **D** (1-methyl-but-2-ynyl acetate) and **T** (1,1-dimethyl-but-2-ynyl acetate) have been used for finding out the mechanism of the reaction.


dx.doi.org/10.1021/jo500822v | J. Org. Chem. 2014, 79, 5652−5663

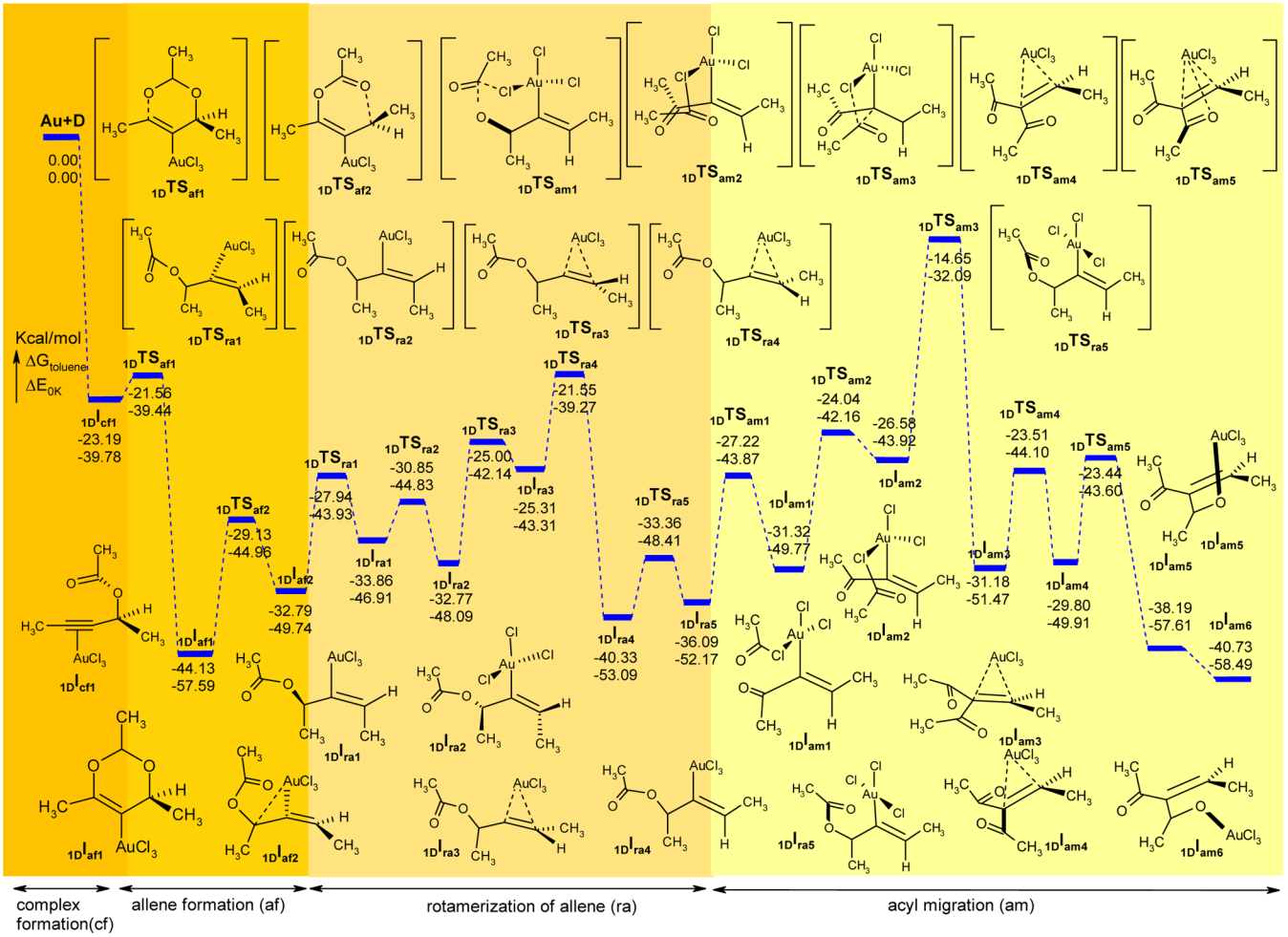


**Figure 2.** PES along with the thermodynamic parameters and structures of the stationary points of path 1 for reactant **D**.

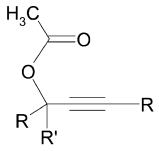

**D**: R=$CH_3$; R'=H
**T**: R=R'=$CH_3$

All the pathways catalyzed by a Au(III) complex were studied using $AuCl_3$ [**Au**]. The overview of all the studied pathways is shown in Figure 1.

The pathways were considered to start with the formation of the coordinate complex of the reactant **D** or **T** with gold salt [**Au**] (deep yellow portion of Figure 1). Three possible sites in the substrate, viz. the C≡C $\pi$ system (indicated by **1** in blue color), the carbonyl oxygen (**2** shown by green color), and the alcoholic oxygen (**3** shown by red color) of the propargylic ester were considered as the possible points for co-ordination. The resulting complexes undergo a [3,3] sigmatropic shift to generate the intermediate gold-bound allene system through the allene formation step (af) (yellow region of Figure 1). In pathway 1 (indicated by blue color), the isomerized allene from the metal bound propergylic ester in its triple bond undergoes a configurational change to juxtapose suitably the migrating acyl group and is designated as rotamerization of allene (ra). The nearly planar structure of the isomerized product further undergoes an acyl migration (am) (light yellow portion in Figure 1) in the form of a monodentate (blue path) or bidentate (deep blue path) complex for generating the diketone. In path 2 (shown by green color in Figure 1), the reactant ester, bonded to the metal in its carbonyl oxygen, undergoes the catalytic rearrangement in two steps; first is the formation of allene (af) followed by the second step of acyl migration (am). Pathway 3 (indicated by red color) utilizes the alcoholic oxygen of the propargylic ester to coordinate with the metal atom and generates the diketone through successive steps such as allene formation (af), rotamerization of allene (ra), and acyl migration (am). Acyl migration may proceed through a monodentate (violet) or bidentate (red) complex of gold. A summary of the activation energies associated with the individual steps and overall processes for all pathways using the substrates **D** and **T** are shown in Table 1. PESs of the energetically most favorable pathway (path 1) for the substrates **D** and **T** are shown in Figures 2 and 3, respectively. Figures with detailed thermodynamic parameters of all the favorable and unfavorable pathways are shown in the Supporting Information. We have used the letters "**I**" and "**TS**" to designate the stationary points for minima and the saddle point, respectively. The subscript on the left side of **I** or **TS** indicates the pathway number followed by the model compound used, while the subscripts in the right side designate the subpath (**cf**, **af**, **ra**, or **am**), under which it belongs, and the species number.

**Analysis of the Investigated Pathways.** The propargylic ester **D** or **T** coordinated by the gold in its triple bond starts the reaction through an internal nucleophilic attack by the carboxylic


dx.doi.org/10.1021/jo500822v | J. Org. Chem. 2014, 79, 5652−5663

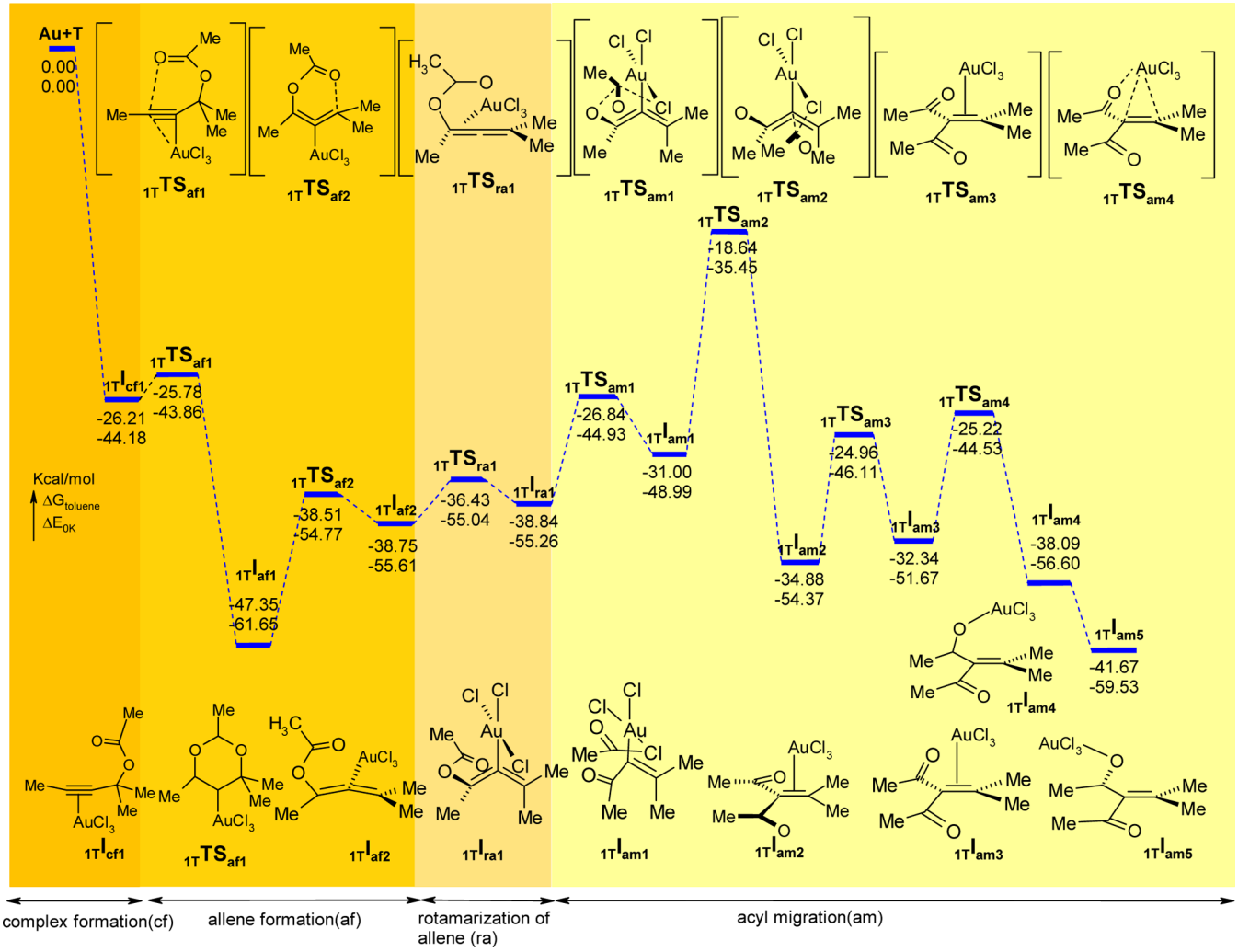


**Figure 3.** PES along with the thermodynamic parameters and structures of the stationary points of path 1 for reactant **T**.

**Scheme 2**

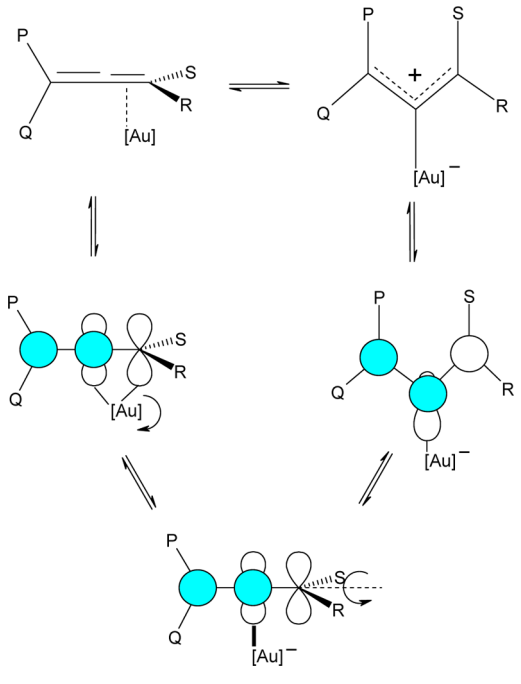


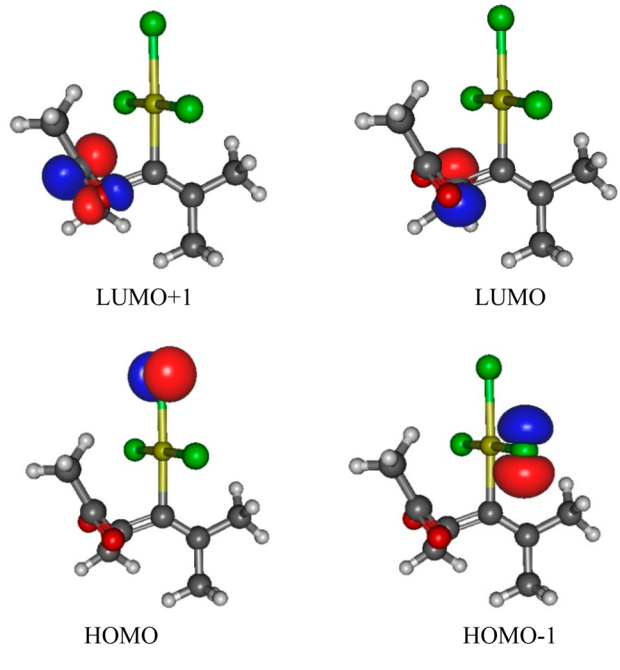


**Figure 4.** Frontier molecular orbitals of $_{1T}I_{ra1}$ intermediate.


dx.doi.org/10.1021/jo500822v | J. Org. Chem. 2014, 79, 5652−5663

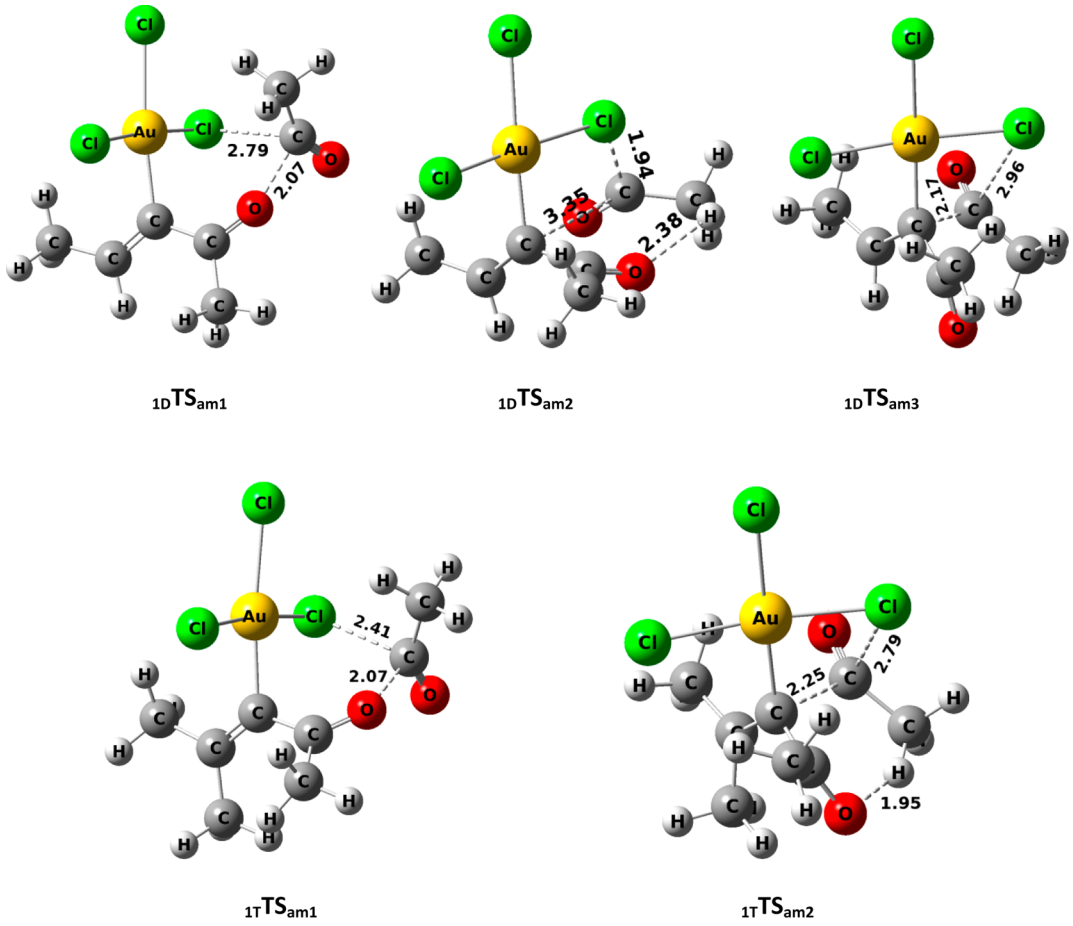


$_{1D}TS_{am1}$ $_{1D}TS_{am2}$ $_{1D}TS_{am3}$

$_{1T}TS_{am1}$ $_{1T}TS_{am2}$

**Figure 5.** Transition structures for the acyl migration step in reactant **D** and **T**.

oxygen atom resulting a six-membered ring intermediate, $_{1D}\mathbf{I}_{af1}$ and $_{1T}\mathbf{I}_{af1}$ (activation energy is about 0.3 kcal mol$^{-1}$; Figure 2 and Figure 3 for **D** and **T**, respectively). The subsequent ring opening to generate the gold-bound allene system occurs by crossing a barrier of 12.6 and 6.9 kcal mol$^{-1}$ (through $_{1D}\mathbf{TS}_{af2}$ and $_{1T}\mathbf{TS}_{af2}$) for **D** and **T** ,respectively. The allene intermediates ($_{1D}\mathbf{I}_{af2}$ and $_{1T}\mathbf{I}_{af2}$), generated by this process, are in the $\eta^2$ form where the gold atom is attached to the proximal double bond of the carboxy allene intermediate. In view to generate the diketone skeleton we have made several attempts to dislocate the acyl group from the acetate oxygen to the central carbon atom of the allenic system; however we failed to get the proper TS that corresponds to the pathway from the reactant allene to product diketone. We observed that some TSs lead to the migration of the acyl group from the oxygen of carboxyallene to one of the chlorine ligand of the metal complex with very low activation barrier. However, the reactant, corresponding to these TSs, needs some extra conformational rearrangement to correlate with the allene, generated from [3,3] rearrangement of propargylic ester. It appeared to us that, the species generated in the allene formation step undergoes a conformational scrambling to attain geometry suitable for further migration of acyl group. Hence, an investigation for pathways to explore the rotamerization of the gold bound allene (ra) has been undertaken before the final step of acyl migration.

We have already mentioned that the metal bound allene complex was reported to be conformationally labile and can readily racemises through planar carbocationic intermediate.[28] The conformational change of gold bound allene complex from its nonplanar allene geometry to the planar one may be looked upon as presented in Scheme 2.

Our observation from the geometry scan revealed that, the oxygen substituent on the allene system stabilizes the planar allyl cation intermediate to a great extent and results a shallow potential energy surface comprising of various configurational arrangement of the structure.[29] Thus, the metal-bound allene system ($_{1D}\mathbf{I}_{af2}$ in Figure 2) for reactant **D** undergoes a conformational change to rotate its acetyl group from its syn to anti conformation and produces a nearly planar $\eta^1$ complex intermediate ($_{1D}\mathbf{I}_{ra1}$). Successive conformational change through a helical intermediate, $_{1D}\mathbf{I}_{ra2}$, results the displacement of the metal atom to the distal double bond on the allenic system, generating an $\eta^2$ complex $_{1D}\mathbf{I}_{ra3}$. Further conformational movement of the terminal methyl group leads to another planar $\eta^1$ complex $_{1D}\mathbf{I}_{ra4}$ in which the two methyl groups at the terminal position of the allenic system are far apart from each other. This geometry then undergoes another conformational change that positions the acetoxy group syn with respect to the allenic system ($_{1D}\mathbf{I}_{ra5}$) and makes it suitable for the final intramolecular acyl migration. Conformational change in trimethyl derivative of allene intermediate ($_{1T}\mathbf{I}_{af2}$ in Figure 3) requires only one TS ($_{1T}\mathbf{TS}_{ra1}$) and does not undergo any syn to anti or anti to syn movement of the acetyl group. The resulting conformer, $_{1T}\mathbf{I}_{ra1}$ juxtaposes suitably the acetoxy group in proper orientation.

After achieving a proper conformation, the acyl migration could take place with the assistance of the chlorine ligand. The participation of the chlorine ligand in the acyl transfer process was first suspected while searching for the TS to dislocate the acyl


dx.doi.org/10.1021/jo500822v | J. Org. Chem. 2014, 79, 5652−5663

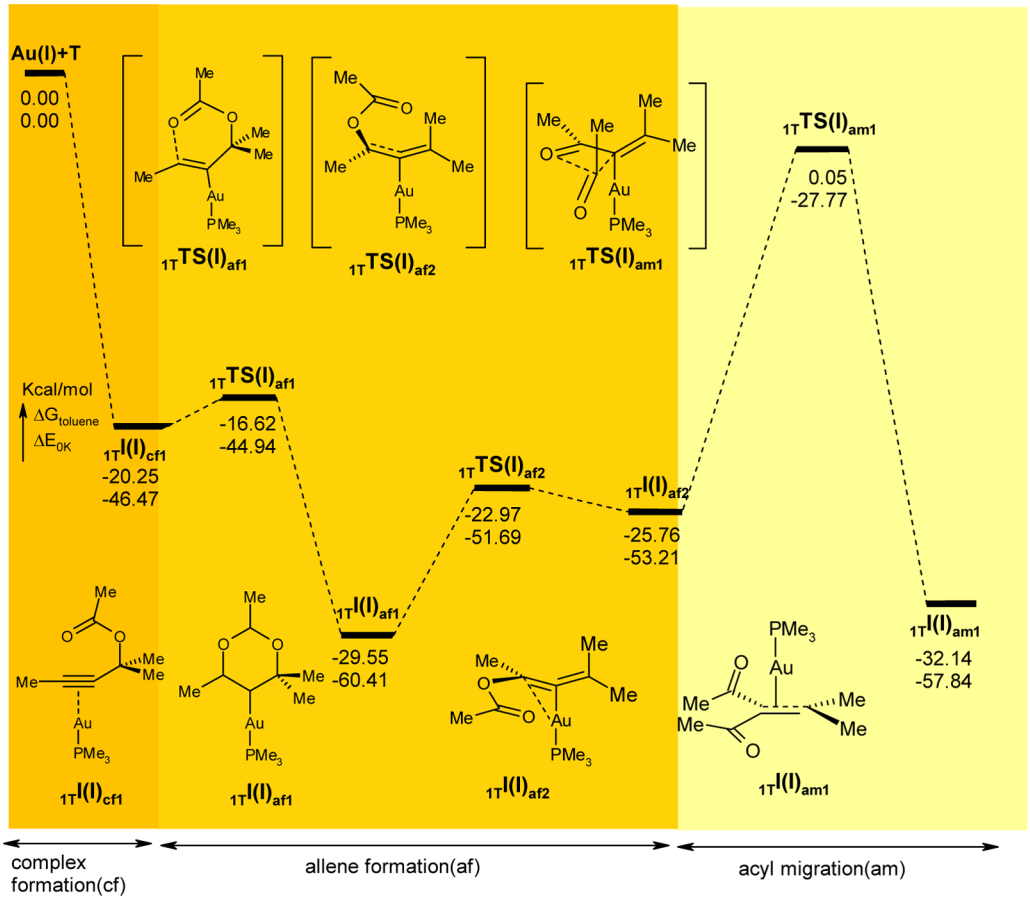


**Figure 6.** PES and the relative energies of the stationary points for the diketone formation from reactant **T** catalyzed by Au(I).

**Table 2. Comparison of Activation Energy (kcal mol$^{-1}$) Required for Au(III)- and Au(I)-Catalyzed Isomerization of Propargylic Esters**

| substrate used | activation barrier for | catalyzed by Au(III) chloride | catalyzed by Au(I) $PMe_3^+$ |
|---|---|---|---|
| **D** | acyl migration (am) | 20.08 (Figure 2) | 26.55 |
| | overall reaction | 25.50 (Figure 2) | 33.83 |
| **T** | acyl migration (am) | 19.81 (Figure 3) | 25.44 (Figure 6) |
| | overall reaction | 26.20 (Figure 3) | 32.64 (Figure 6) |

group to generate the diketone skeleton. However, it can be justified by the analysis of the frontier MOs associated with any of the intermediate, $_{1D}I_{ra5}$ and $_{1T}I_{ra1}$ (Figure 4 shows only the frontier MOs of $_{1T}I_{ra1}$).

As evident from Figure 4, the vacant LUMO+1 orbital of $_{1T}I_{ra1}$ is associated with the carbon atom of the carbonyl group in migrating acyl unit, while the occupied MOs (HOMO or HOMO−1) in the outer sphere of the system are associated with the chlorine atoms that acts as the ligand of the metal ion. This arrangement of the orbitals suggests that the migrating acyl group prefers to attach itself to the chlorine in the first step; in the next step, it migrates to its final destination of the carbon atom bonded to the gold ion. Hence, the chlorine, placed at the vicinity of the acyl group (in $_{1D}I_{ra5}$ and $_{1T}I_{ra1}$), mediates the shifting process by acting as a *platform atom* during the journey of acyl

**Scheme 3**

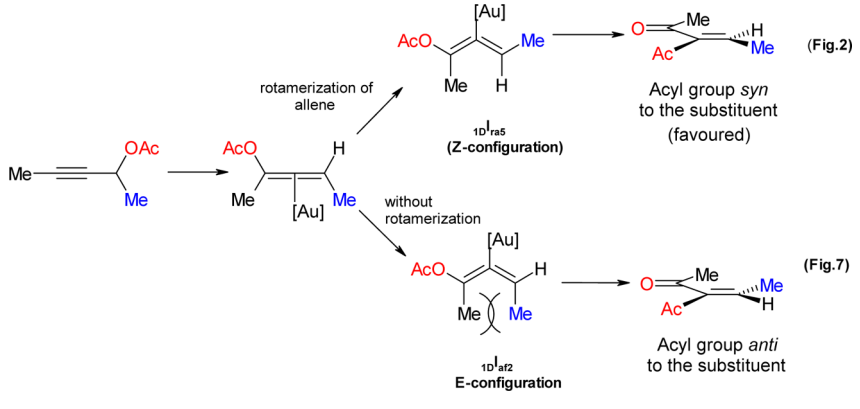



dx.doi.org/10.1021/jo500822v | J. Org. Chem. 2014, 79, 5652−5663

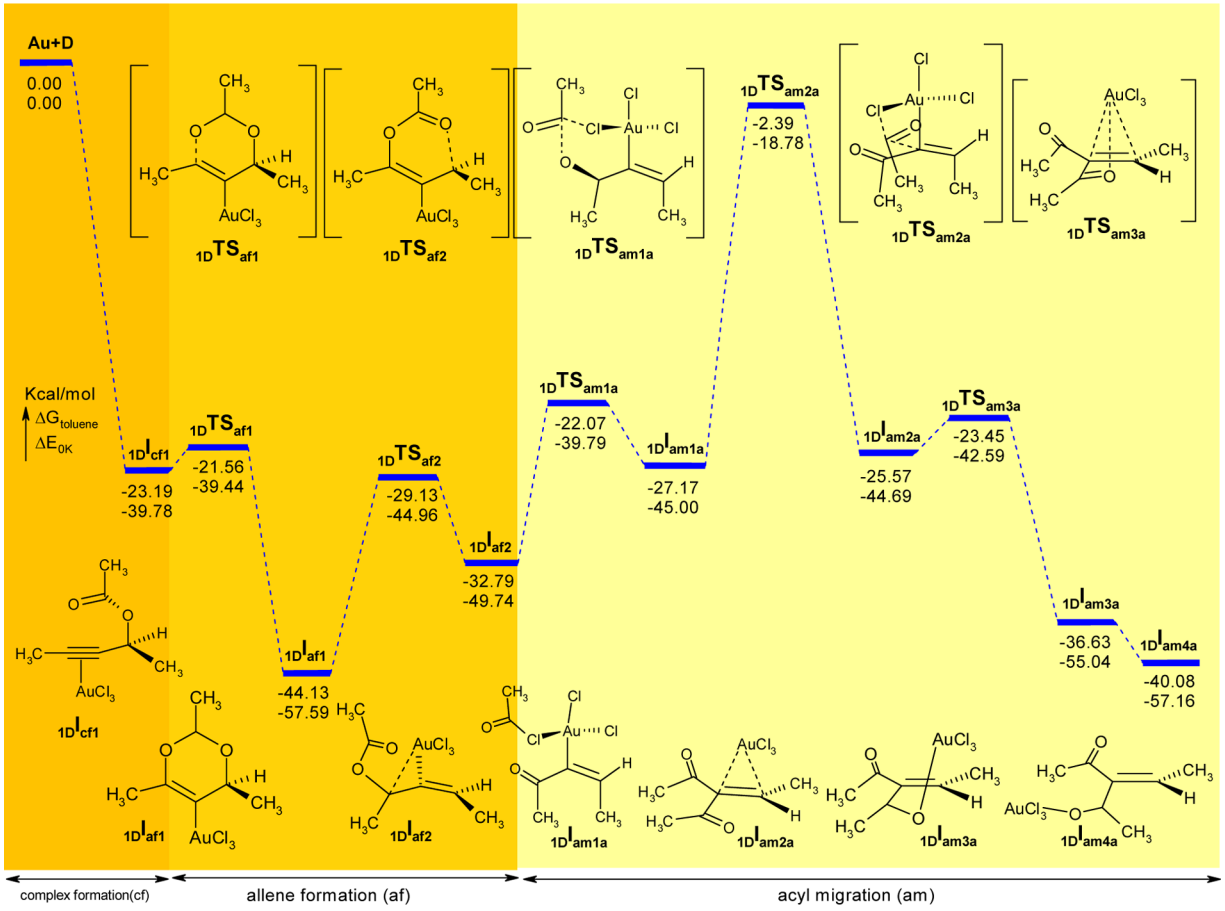


**Figure 7.** PES along with the thermodynamic parameters and structures of the stationary points of diastereomeric path 1 (without any rotamerization) for reactant **D**.

group from the oxygen to the carbon atom. This process results two TSs for the overall migration of acyl group; the first one results from the migration of acyl group to the chlorine, while the second TS corresponds to the migration from chlorine to the middle carbon of the allene system.

The allene-bound gold complexes $_{1D}\mathbf{I}_{ra5}$ and $_{1T}\mathbf{I}_{ra1}$ (for reactant **D** and **T** respectively, Figure 2 and 3) undergo the first step of acyl migration to form $_{1D}\mathbf{I}_{am1}$ and $_{1T}\mathbf{I}_{am1}$ through the TSs $_{1D}\mathbf{TS}_{am1}$ and $_{1T}\mathbf{TS}_{am1}$ with an activation barrier of 8.30 and 10.33 kcal mol$^{-1}$, respectively. While forming the TSs, the distance of the carbonyl carbon of the migrating acyl group from the detached oxygen atom is 2.07 Å in both $_{1D}\mathbf{TS}_{am1}$ and $_{1T}\mathbf{TS}_{am1}$ (Figure 5). However, the distance of the same one from the chlorine ligand varies slightly (2.79 Å in $_{1D}\mathbf{TS}_{am1}$ and 2.41 Å in $_{1T}\mathbf{TS}_{am1}$). The resultant intermediates ($_{1D}\mathbf{I}_{am1}$ in Figure 2 and $_{1T}\mathbf{I}_{am1}$ in Figure 3) show a new bond between the chlorine ligand and carbon atom of the migrated acyl group. Further migration of the acyl group in the second step of the movement in reactant **T** forms a new C−C bond (through $_{1T}\mathbf{TS}_{am2}$; activation barrier 13.54 kcal mol$^{-1}$) and generates the skeleton of the product diketone (Figure 3). The last step that involves the formation of carbon−carbon bond is the energetically most costly step (and hence the rate limiting step) in the overall rearrangement process. Reactant **D** requires an additional step, in between the two acyl migration processes, that makes a conformational change in the intermediate $_{1D}\mathbf{I}_{am1}$ to generate $_{1D}\mathbf{I}_{am2}$ (through $_{1D}\mathbf{TS}_{am2}$ with activation energy 7.61 kcal mol$^{-1}$, Figure 2). Intermediate $_{1D}\mathbf{I}_{am2}$ finally rearranges through a rate-limiting step to $_{1D}\mathbf{I}_{am3}$ (activation barrier 11.83 kcal mol$^{-1}$) in which the Au atom is coordinated to the C═C double bond. During the migration of the acyl group, the conformation of the newly formed carbonyl group at the terminal of allene skeleton changes from the syn periplanar position to the anti one with respect to the Au atom (Figure 5). Species $_{1D}\mathbf{I}_{am3}$ and $_{1T}\mathbf{I}_{am2}$ (Figure 2 and 3) are further stabilized after transferring the Au atom from the C═C double bond to the lone pair of oxygen atom of one ketone group. The activation barrier, summarized in Table-1, shows that the energy required for overall acyl migration process in **D** and **T** are nearly equal (20.08 and 19.81 kcal mol$^{-1}$). Incorporation of the dispersion correction lowers this activation barrier to a small extent (18.87 and 18.23 kcal mol$^{-1}$). During analysis of the energies of the pathway we calculated the solvent effect; however, no appreciable change has been noticed, which indicates the solvent has little effect on the reaction rate.

The possibility of the formation of bidentate complex in the rotamerized allene before the acyl migration step has also been examined. However, our computation reveals that the formation of chelate complex by replacing one chlorine atom in the Au complex requires a high activation energy and appears to be a highly unfavorable process (the energy of the TS corresponding to the chelate formation step is shown in the Supporting Information). Further investigation on paths 2 and 3 (monodentate and bidentate complex formation) reveals that the activation energies associated with these paths are relatively high (Table 1). Detailed PES, analysis, and scheme are shown in the Supporting Information.


dx.doi.org/10.1021/jo500822v | J. Org. Chem. 2014, 79, 5652−5663

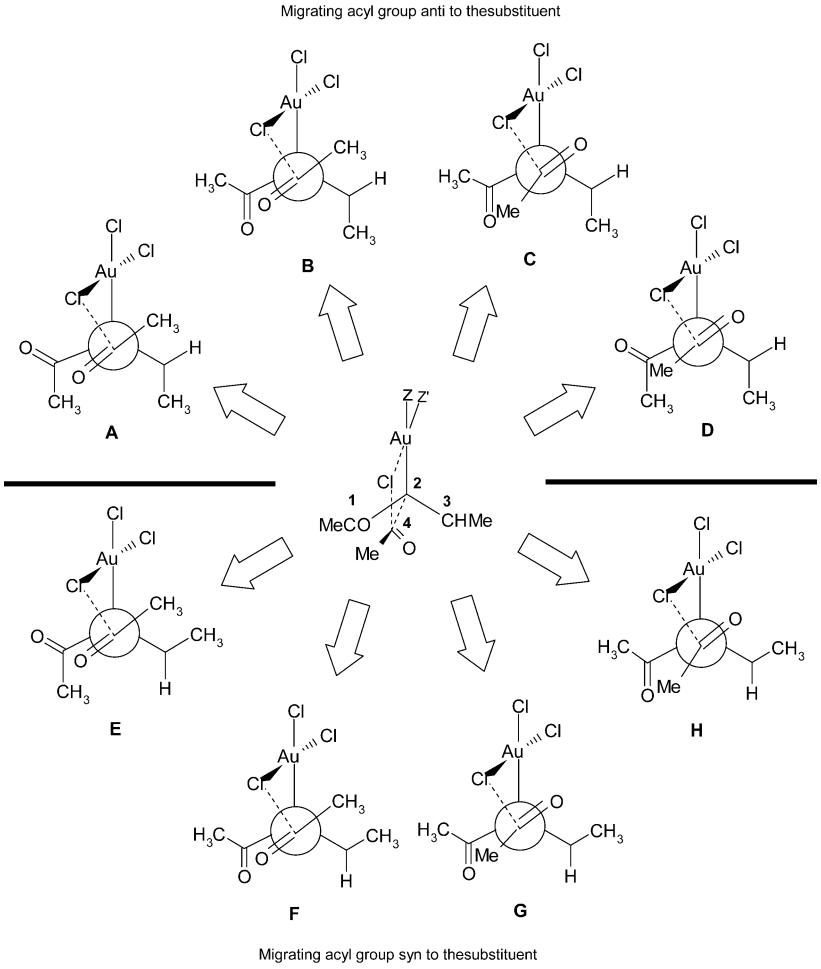


**Figure 8.** Possible conformers of the transition state associated with the rate-limiting process.

Comparison of the reaction pathways corresponding to the three coordinated complexes of the propargylic ester with gold salt (Figure 1 and Table 1) suggests that path 1 (through monodentate complex formation of the metal ion) is the most preferred for both **D** and **T** since the highest energy transition state along this pathway is much lower in energy than the highest energy transition state along the other pathways. Based on the energy values shown in Table 1, we have considered path 1 as the plausible mechanism and employed it for our all successive discussions to rationalize the other consequences associated with the reaction.

**Catalysis under Au(I) Metal Ion.** The effectiveness of the Au(I) salt as a catalyst to carry out the isomerization of propargylic ester to diketone has also been investigated. A qualitative explanation of its reduced activity, as observed in the experimental report,[3] may be put forward if we consider the critical role of the chlorine ligand in the most favorable pathway (path 1) for Au(III)-catalyzed conditions as discussed in the previous sections. In its linear geometry, the Au(I) metal complex is unable to place the assisting ligand in suitable orientation which can participate in the catalytic process for migration of the acyl group. We have verified the energetically costly direct migration of acyl group from the oxygen to the central $sp^2$-hybridized carbon atom in Au(I) catalyzed isomerization of **T** as shown in Figure 6.

The Au(I)-bound complex ${}_{1T}\mathbf{I(I)}_{cf1}$ undergoes the formation of the six-membered intermediate ${}_{1T}\mathbf{I(I)}_{af1}$, through the internal nucleophilic attack of the carbonyl oxygen to the terminal alkyne carbon atom (${}_{1T}\mathbf{TS(I)}_{af1}$). Ring-opening and rotamerization of the allene complex occur in a single step through ${}_{1T}\mathbf{TS(I)}_{af2}$ and generate the intermediate ${}_{1T}\mathbf{I(I)}_{af2}$. The latter intermediate, without any further conformational change, rearranges to ${}_{1T}\mathbf{I(I)}_{am1}$ by a single-step acyl migration process through ${}_{1T}\mathbf{TS(I)}_{am1}$. Without a detailed similar study for substrate **D**, we have calculated only the activation barrier of the rate-limiting step of the overall pathway for Au(I)-catalyzed isomerization of the substrate **D** and compared them with that of he reaction catalyzed by Au(III) salt (Table 2). In all cases, the activation barrier required for Au(I)-catalyzed processes shows a higher value than that observed for Au(III)-catalyzed processes and thus justifies the experimental facts for the reduced activity of lower oxidation state of the metal ion again.

**Stereoselectivity.** The experimental report[3] shows that the *E*-selectivity is the initial outcome of the propargylic ester rearrangement process, though lengthening the reaction time results in an erosion of the stereoselectivity. A closer look at the product selectivity reveals that the mechanistic path 1 (most favorable pathway) can produce the same selectivity and it is due to the electrophilic attack on the *Z*-configuration of the Au(III) vinyl complex (${}_{1D}\mathbf{I}_{ra5}$ in Figure 2 and Scheme 3). This isomer of gold-bound allene complex is generated from the diastereomeric ${}_{1D}\mathbf{I}_{af2}$ intermediate through rotamerization (Figure 2). Without going through such a rotamerization step, the acyl migration generates the product by electrophilic attack on the diastereomeric


dx.doi.org/10.1021/jo500822v | J. Org. Chem. 2014, 79, 5652−5663

**Table 3. Relative Energies of Different Configurations of the Optimized Geometries of the Rate Determining Transition Structure (Figure 8)**

| | | configurations leading to acyl migration *anti* to the substituent | | | | configurations leading to acyl migration *syn* to the substituent | | | |
|---|---|---|---|---|---|---|---|---|---|
| | | A | B | C | D | E | F | G | H |
| $AuCl_3$ (Z = Z′ = Cl in Figure 8) | | | | | | | | | |
| C1−C2 | | ±sp | ±ap | ±ap | ±sp | ±sp | ±ap | ±ap | −ac |
| C2−C3 | | ±ap | ±ap | ±ap | ±ap | ±sp | ±sp | ±sp | ±sp |
| C2−C4 | | +ac | +ac | −sc | −sc | +ac | +ac | −sc | −sc |
| | | | | | $_{1D}$**TS**$_{am2a}$ | | | $_{1D}$**TS**$_{am3}$ | |
| | $\Delta G_{toluene}^{\ddagger}$ | 9.58 | | | 12.26 | 6.16 | | 0.00 | 3.68 |
| | $\Delta G_{353}^{\ddagger}$ | 10.34 | | | 12.72 | 7.53 | | 0.00 | 3.66 |
| | $\Delta H_{353}^{\ddagger}$ | 10.59 | | | 13.36 | 7.25 | | 0.00 | 4.74 |
| | $\Delta E_0^{\ddagger}$ | 10.57 | | | 13.31 | 7.28 | | 0.00 | 4.54 |
| PicAuCl$^+$ (Z, Z′ = Pic in Figure 8) | | | | | | | | | |
| C1−C2 | | ±sp | ±ap | ±ap | ±sp | ±sp | ±ap | ±ap | -ac |
| C2−C3 | | ±ap | ±ap | ±ap | ±ap | ±sp | ±sp | ±sp | ±sp |
| C2−C4 | | +ac | +ac | −sc | −sc | +ac | +ac | −sc | −sc |
| complex in configuration SP-4-2 | $\Delta G_{toluene}^{\ddagger}$ | 6.20 | 2.35 | 1.27 | 7.86 | 3.24 | 2.13 | 0.00 | 3.06 |
| | $\Delta G_{353}^{\ddagger}$ | 8.02 | 3.73 | 1.24 | 9.45 | 4.89 | 3.18 | 0.00 | 3.55 |
| | $\Delta H_{353}^{\ddagger}$ | 9.67 | 5.21 | 1.83 | 10.83 | 5.62 | 3.51 | 0.00 | 4.87 |
| | $\Delta E_0^{\ddagger}$ | 9.36 | 4.86 | 1.71 | 10.59 | 5.42 | 3.44 | 0.00 | 4.67 |
| C1−C2 | | +ac | +ac | ±ap | ±sp | ±sp | ±ap | ±ap | ±sp |
| C2−C3 | | ±ap | ±ap | ±ap | ±ap | ±sp | ±sp | ±sp | ±sp |
| C2−C4 | | +ac | +ac | -ac | -ac | +ac | +ac | −sc | -ac |
| complex in configuration SP-4-3 | $\Delta G_{toluene}^{\ddagger}$ | 13.32 | 13.32 | 18.16 | 16.24 | 13.49 | 11.85 | 11.67 | 12.95 |
| | $\Delta G_{353}^{\ddagger}$ | 17.37 | 17.37 | 22.27 | 19.67 | 18.20 | 16.63 | 15.81 | 16.74 |
| | $\Delta H_{353}^{\ddagger}$ | 16.93 | 16.93 | 22.35 | 21.45 | 18.84 | 16.68 | 15.49 | 17.06 |
| | $\Delta E_0^{\ddagger}$ | 17.05 | 17.05 | 22.35 | 21.20 | 18.70 | 16.75 | 15.62 | 16.99 |

*E*-configuration of the Au(III) vinyl complex (Scheme-3), and the PES is presented in Figure 7.

Comparison of PES of Figure 7 with Figure 2 reveals that the intermediate $_{1D}$**I**$_{af2}$ generated after [3,3] shift of the acetate unit undergoes an acyl migration through two successive movement of the acyl group; first from O to Cl with activation barrier of 9.95 kcal mol$^{-1}$ (through $_{1D}$**TS**$_{am1a}$) and then from Cl to allenic C carbon with a barrier of 26.22 kcal mol$^{-1}$ (though $_{1D}$**TS**$_{am2a}$). The overall high energy barrier in acyl migration step ($_{1D}$**TS**$_{am2a}$ with activation barrier 30.96 kcal mol$^{-1}$) clearly shows that this diastereomeric pathway (Figure 7) is unfavorable and supports the stereoselectivity as indicated in the experimental result. To ascertain about the involvement of other possible isomeric TS in contributing the overall diastereoselectivity we have made an exhaustive search on the possible conformational geometries (Figure 8) of the rate-limiting transition structure, $_{1D}$**TS**$_{am3}$. The relative energy values of the optimized geometries with their conformations are shown in Table 3. We failed to get the optimized geometry corresponding to the conformer **B**, **C**, and **F**; however, relative energy (Table 3) of other conformers reveals that **G** (which is the same species as $_{1D}$**TS**$_{am3}$) represent the most stable member. All the species that lead to the *Z* product (**A**−**D**) show the antiperiplanar conformation of the C2−C3 bond. On the other hand, the *E* selectivity is produced by the syn periplanar arrangement of the methyl group with respect to metal atom in C2−C3 bond (**E**−**H**). It is apparent from the energy values that the syn conformations that lead to the *E*-isomer are more favorable than the conformer having anti arrangement. The steric interaction between the methyl group at C3 and the groups connected to C1 in an anti arrangement (**A**−**D** in Figure 8) are probably the reason behind the instability of such conformers. Involvement of a more sophisticated catalyst has also been examined as the experimental report shows a better selectivity by using the catalyst $PicAuCl_2$. While examining the transition structure involving the species **PicAuCl**$^+$, we identified two possible orientations SP-4-2 and SP-4-3 (the descriptors[30] have been chosen to designate the orientation of the pyridinium ring and carboxylate oxygen with respect to the chlorine ligand) of the catalyst in each conformer of Figure 8.

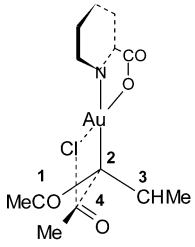

SP-4-2

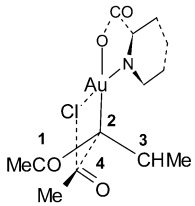

SP-4-3

As shown in Table 3, conformer **A** and **B** in SP-4-3 metal complex optimize to the same minima. The relative energy of all these species reveals that catalyst prefers the SP-4-2 isomeric orientation relative to the substrate and the isomer **G** represents the most stable species among all.

## CONCLUSION

In summary, our DFT study establishes that the isomerization of propargylic ester to a diketone derivative under the catalysis of Au(III) metal salt takes place in three tandem rearrangement steps (Figure 9). The first step involves the [3,3] sigmatropic rearrangement of the metal-bound propargylic ester to a metal-bound allene intermediate. In the next step, the generated carboxyallene derivative undergoes a conformational scrambling


dx.doi.org/10.1021/jo500822v | J. Org. Chem. 2014, 79, 5652−5663

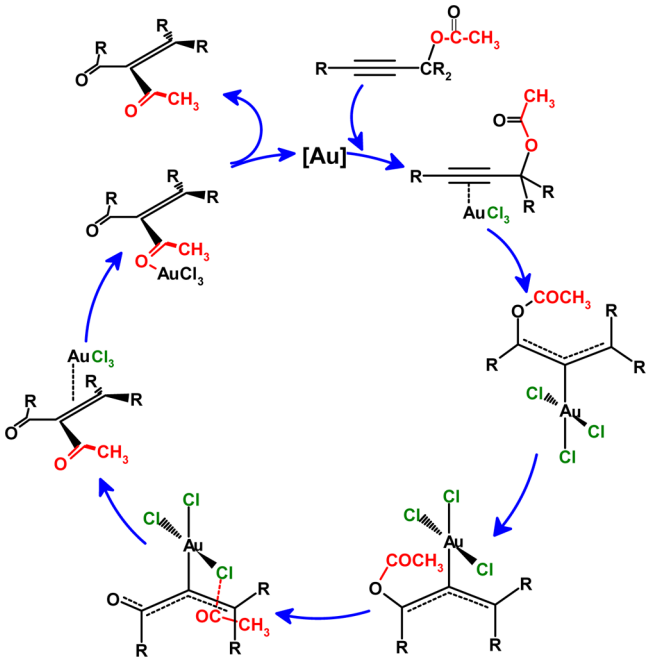


**Figure 9.** Overall catalytic cycle for conversion of propargylic ester to diketone.

that orients the acyl group, to be migrated, in a proper position close to a metal ligand chlorine atom. After attaining at a suitable conformational state, the species, in the third step, rearranges by an intramolecular acyl migration from the acetate oxygen to the chlorine ligand. The resulting species on further movement of acyl group from chlorine to the central carbon of the allene system results in the diketone skeleton.

The movement of the acyl group from ligand chlorine to the carbon atom has been identified as the rate-limiting step and necessarily occurs through a specific low energy TS that dictates the final stereoselectivity of the reaction. Being a linear structure, the Au(I) metal salt cannot assist the migration in a similar fashion. This fact justifies the reduced effectiveness of Au(I) salt to carry out the isomerization reaction under similar conditions. While analyzing the diastereoselectivity, it appeared to us that the best conformational arrangement of the transition structure that dictates the final diastereoselectivity of the products is suffering from minimal steric interaction between the substituent methyl groups present in the substrate of propargylic ester. The changing of the steric and electronic nature of these substituents may alter the stereoselectivity as observed experimentally by other group while examining the same reaction with a different substrate under several metal catalytic conditions.[31] Study on the alternation of diastereoselectivity with the variation of substituents present in the propargylic ester is our future objective. It is our belief that the outcome of this study, i.e., involvement of a ligand to catalyze the isomerization process, will further promote the experimentalists to design suitable catalyst for increasing its efficiency and selectivity.

## ■ ASSOCIATED CONTENT

### Supporting Information

PES of all pathways, Cartesian coordinates, absolute energies, frequencies, and detailed thermodynamic parameters for all the computed stationary points along with the structure and ball and stick model. This material is available free of charge via the Internet at http://pubs.acs.org.

## ■ AUTHOR INFORMATION

### Corresponding Author

*E-mail: gourabkanti.das@visva-bharati.ac.in.

### Notes

The authors declare no competing financial interest.

## ■ ACKNOWLEDGMENTS

All the authors are thankful to the UGC, New Delhi, India, for providing financial assistance in the form of an MRP [no. 41-207/2012(SR)]. One of us (A.G.) thanks UGC for a BSR Research Fellowship [no. F.4-1/2006(BSR)/7-199/2007(BSR)] . K.C. is thankful to CSIR, New Delhi, India, for a Senior Research Associateship [no. 13(8631-A)/2013-Pool].

## ■ REFERENCES

(1) Acyl migration takes place from O to C atom in aromatic system by Fries rearrangement: (a) Fries, K.; Finck, G. *Ber.Dtsch. Chem. Ges.* **1908**, *41*, 4271. (b) For recent reviews see: Sartori, G.; Maggi, R. *Chem. Rev.* **2011**, *111*, PR181−PR214.

(2) For a recent review on allene and its reaction see: Soriano, E.; Fernandez, I. *Chem. Soc. Rev.* **2014**, DOI: 10.1039/c3cs60457h.

(3) Wang, S.; Zhang, L. *J. Am. Chem. Soc.* **2006**, *128*, 8414−8415.

(4) For reviews on gold catalysis: (a) Hashmi, A. S. K.; Rudolph, M. *Chem. Soc. Rev.* **2008**, *37*, 1766. (b) Gorin, D. J.; Sherry, B. D.; Toste, F. D. *Chem. Rev.* **2008**, *108*, 3351. (c) Arcadi, A. *Chem. Rev.* **2008**, *108*, 3266. (d) Fürstner, A.; Davies, P. W. *Angew. Chem., Int. Ed.* **2007**, *46*, 3410. (e) Díez-González, S.; Marion, N.; Nolan, S. P. *Chem. Rev.* **2009**, *109*, 3612. (f) Hashmi, A. S. K. *Chem. Rev.* **2007**, *107*, 3180. (g) Nolan, S. P. *Acc. Chem. Res.* **2011**, *44*, 91. (h) Wang, S.; Zhang, G.; Zhang, L. *Synlett* **2010**, 692. (i) Patil, N. T.; Yamamoto, Y. *Chem. Rev.* **2008**, *108*, 3395. (j) Li, Z.; Brouwer, C.; He, C. *Chem. Rev.* **2008**, *108*, 3239. (k) Jiménez-Núñez, E.; Echavarren, A. M. *Chem. Rev.* **2008**, *108*, 3326.

(5) (a) Marion, N.; Nolan, S. P. *Angew. Chem., Int. Ed.* **2007**, *46*, 2750. (b) Marco-Contelles, J.; Sorjano, E. *Chem.—Eur. J.* **2007**, *13*, 1350.

(6) Correa, A.; Marion, N.; Fensterbank, L.; Malacria, M.; Nolan, S. P.; Cavallo, L. *Angew. Chem., Int. Ed.* **2008**, *47*, 718.

(7) Li, G.; Zhang, G.; Zhang, L. *J. Am. Chem. Soc.* **2008**, *130*, 3740.

(8) (a) Miki, K.; Ohe, K.; Uemura, S. *J. Org. Chem.* **2008**, *68*, 8505. (b) Mamane, V.; Gress, T.; Krause, H.; Fürstner, A. *J. Am. Chem. Soc.* **2004**, *126*, 8654. (c) Shi, X.; Gorin, D. J.; Toste, F. D. *J. Am. Chem. Soc.* **2005**, *127*, 5802. (d) Johansson, M. J.; Gorin, D. J.; Staben, S. T.; Toste, F. D. *J. Am. Chem. Soc.* **2005**, *127*, 18002.

(9) (a) Zhang, L. *J. Am. Chem. Soc.* **2005**, *127*, 16804. (b) Zhang, L.; Wang, S. *J. Am. Chem. Soc.* **2006**, *128*, 1442. (c) Buzas, A.; Istrate, F.; Gagosz, F. *Org. Lett.* **2006**, *8*, 1957. (d) Wang, S.; Zhang, L. *Org. Lett.* **2006**, *8*, 4585. (e) Buzas, A.; Gagosz, F. *J. Am. Chem. Soc.* **2006**, *128*, 12614. (f) Wang, S.; Zhang, L. *J. Am. Chem. Soc.* **2006**, *128*, 14274. (g) Garayalde, D.; Gomez-Bengoa, E.; Huang, X.; Goeke, A.; Nevado, C. *J. Am. Chem. Soc.* **2010**, *132*, 4720.

(10) (a) Marion, N.; Díez-González, S.; Frémont, P.; Noble, A. R.; Nolan, S. P. *Angew. Chem., Int. Ed.* **2006**, *45*, 3647. (b) Marion, N.; Carlqvist, P.; Gealageas, R.; Fremont, P.; Maseras, F.; Nolan, S. P. *Chem.−Eur. J.* **2007**, *13*, 6437. (c) Dudnik, A. S.; Sromek, A. W.; Rubina, M.; Kim, J. T.; Kel'in, A. V.; Gevorgyan, V. *J. Am. Chem. Soc.* **2008**, *130*, 1440. (d) Döpp, R.; Lothschütz, C.; Wurm, T.; Pernpointer, M.; Keller, S.; Rominger, F.; Hashmi, A. S. K. *Organometallics* **2011**, *30*, 5894.

(11) (a) Cran, J. W.; Krafft, M. E. *Angew. Chem.* **2012**, *124*, 9532. (b) Hashmi, A. S. K.; Schwarz, L.; Choi, J.-H.; Frost, T. M. *Angew. Chem., Int. Ed.* **2000**, *39*, 2285. (c) Alfonsi, M.; Arcadi, A.; Aschi, M.; Bianchi, G.; Marinelli, F. *J. Org. Chem.* **2005**, *70*, 2265.

(12) (a) Hashmi, A. S. K.; Schwarz, L.; Rubenbauer, P.; Blanco, M. C. *Adv. Synth. Catal.* **2006**, *348*, 705. (b) Hashmi, A. S. K.; Ramamurthi, T. D.; Rominger, F. *J. Organomet. Chem.* **2009**, *694*, 592.

(13) Effect of the oxidation state of the gold ion on the course of reaction has been reported several times: (a) A reversed regioselectivity has been pointed out for the intermolecular hydroarylation of alkynes with arenes under Au(I) catalysis as opposed to Au(III): Nevado, C.;

Echavarren, A. M. *Synthesis* **2005**, 167. (b) Gevorgyan et. al. showed a divergent product formation under the catalysis of each oxidation state. Product under Au(I) catalysis reveals an initial activation of allene, whereas the product formed by Au(III) catalyst is consistent with activation of the ketone moiety: Sromek, A. W.; Rubina, M.; Gevorgyan, V. *J. Am. Chem. Soc.* **2005**, *127*, 10500. (c) Calculation by Straub reveals that the catalyst $AuCl_3$ prefers to coordinate the aldehydic oxygen over alkyne one by 5.10 kcal $mol^{-1}$, though it can catalyze the reaction by activating an alkyne bond: Straub, B. F. *Chem. Commun.* **2004**, 1726.

(14) In their first attempt, the authors found a mixture of isomeric product with some excess in *Z* isomer. Further experiments after optimizing the reaction conditions with the variation of reaction time and catalyst showed that reaction le to the product with *E* selectivity, which on further processing is converted to a mixture of both isomers, and the ratio of the diastereomeric products depends on the thermodynamic stability of the individual isomers.

(15) (a) Conformational mobility and the reactivity of the metal-bound product, generated from the [2,3] or [3,3] rearrangement of propargylic ester, have been reported several times by researchers. While studying the gold(I)-catalyzed Rautenstrauch rearrangement of 1-ethynyl-2-propenyl acetates to cylopentenones, Toste and co-workers observed a remarkable chirality transfer from the substrate to the product: Shi, X.; Gorin, D. J.; Toste, F. D. *J. Am. Chem. Soc.* **2005**, *127*, 5802−5803. (b) Theoretical study of the mechanism reveals that the process involves a center-to-helix-to-center chirality transfer and the helix chirality of the pentadienyl cation does not get the opportunity to undergo racemization process as it is converted to the product by crossing a relatively low energy barrier of cylopentannelation: Faza, O. N.; López, C. S.; Álvarez, R.; de Lera, A. R. *J. Am. Chem. Soc.* **2006**, *128*, 2434−2437. However, moderate chirality transfer as well as loss of chirality has been observed in the allene reaction catalyzed by gold. (c) Gandon, V.; Lemi_ere, G.; Hours, A.; Fensterbank, L.; Malacria, M. *Angew. Chem., Int. Ed.* **2008**, *47*, 7534. (d) Mauleón, P.; Krinsky, J. L.; Toste, F. D. *J. Am. Chem. Soc.* **2009**, *131*, 4513. (e) González, A. Z.; Benitez, D.; Thatchouk, E.; Goddard, W. A.; Toste, F. D. *J. Am. Chem. Soc.* **2011**, *133*, 5500.

(16) Malacria, M.; Fensterbank, L.; Gandon, V. *Top. Curr. Chem.* **2011**, *302*, 157.

(17) (a) Eisenstein, O.; Hoffmann, R. *J. Am. Chem. Soc.* **1981**, *103*, 4308. (b) Senn, H. M.; Blöchl, P. E.; Togni, A. *J. Am. Chem. Soc.* **2000**, *122*, 4098.

(18) Chenier, H. H. B.; Howard, J. A.; Mile, B. *J. Am. Chem. Soc.* **1985**, *107*, 4190.

(19) For example, see: Zhang, Z.; Bender, C. F.; Widenhoefer, R. A. *J. Am. Chem. Soc.* **2007**, *129*, 14148.

(20) Basak, A.; Chakrabarty, K.; Ghosh, A.; Das, G. K. *J. Org. Chem.* **2013**, *78*, 9715.

(21) Kang, R.; Chen, H.; Shaik, S.; Yao, J. *J. Chem. Theory Comput.* **2011**, *7*, 4002.

(22) (a) Hay, P. J.; Wadt, W. R. *J. Chem. Phys.* **1985**, *82*, 270. (b) Wadt, W. R.; Hay, P. J. *J. Chem. Phys.* **1985**, *82*, 284. (c) Hay, P. J.; Wadt, W. R. *J. Chem. Phys.* **1985**, *82*, 299.

(23) (a) Ditchfield, R.; Hehre, W. J.; Pople, J. A. *J. Chem. Phys.* **1971**, *54*, 724. (b) Hehre, W. J.; Ditchfield, R.; Pople, J. A. *J. Chem. Phys.* **1972**, *56*, 2257. (c) Hariharan, P. C.; Pople, J. A. *Theor. Chim Acta* **1973**, *28*, 213. (d) Hariharan, P. C.; Pople, J. A. *Mol. Phys.* **1974**, *27*, 209. (e) Dill, J. D.; Pople, J. A. *J. Chem. Phys.* **1975**, *62*, 2921. (f) Francl, M. M.; Petro, W. J.; Hehre, W. J.; Binkley, J. S.; Gordon, M. S.; DeFrees, D. J.; Pople, J. A. *J. Chem. Phys.* **1982**, *77*, 3654. (g) Rassolov, V. A.; Pople, J. A.; Ratner, M. A.; Windus, T. L. *J. Chem. Phys.* **1998**, *109*, 1223.

(24) Tomasi, J.; Persico, M. *Chem. Rev.* **1994**, *94*, 2027.

(25) Frisch, M. J. et al. Gaussian 09, revision C.01, Gaussian Inc., Wallingford CT, 2010. (Full reference is given in SI).

(26) (a) Grimme, S.; Antony, J.; Ehrlich, S.; Krieg, H. *J. Chem. Phys.* **2010**, *132*, 154104. (b) Kruse, H.; Goerigk, L.; Grimme, S. *J. Org. Chem.* **2012**, *77*, 10824.

(27) (a) Grimme, S.; Ehrlich, S.; Goerigk, L. *J. Comput. Chem.* **2011**, *32*, 1456. See also: (b) Becke, A. D.; Johnson, E. R. *J. Chem. Phys.* **2005**, *122*, 154101. (c) Johnson, E. R.; Becke, A. D. *J. Chem. Phys.* **2005**, *123*, 024101. (d) Johnson, E. R.; Becke, A. D. *J. Chem. Phys.* **2006**, *124*, 174104.

(28) (a) Faza, O. N.; López, C. S.; Álvarez, R.; de Lera, A. R. *J. Am. Chem. Soc.* **2006**, *128*, 2434. (b) Wang, Y.-M.; Kuzniewski, C. N.; Rauniyar, V.; Hoong, C.; Toste, F. D. *J. Am. Chem. Soc.* **2011**, *133*, 12972. (c) Wang, D.; Gautam, L. N.; Bollinger, C.; Harris, A.; Li, M.; Shi, X. *Org. Lett.* **2011**, *13*, 2618.

(29) A detailed PES of the conformational mobility of $AuCl_3$ bound allene intermediates (both substituted and unsubstituted) has been analyzed and presented in the Supporting Information (Figure.SI-12).

(30) Connelly, N. G.; Damhus, T.; Hartshorn, R. M.; Hutton, A. T. In *Nomenclature of Inorganic Chemistry*; IUPAC recommendations 2005, International Union of Pure and Applied Chemistry; Royal Society Publishing: London, 2005.

(31) Barluenga, J.; Riesgo, L.; Vicente, R.; López, L. A.; Tomas, M. *J. Am. Chem. Soc.* **2007**, *129*, 7772.